X-ray absorption and diffraction studies of the mixed-phase state of $(Cr_xV_{1-x})_2O_3$

D. M. Pease,[1,*] A. I. Frenkel,[2,†] V. Krayzman,[3,4,‡] T. Huang,[1] P. Shanthakumar,[1] J. I. Budnick,[1] P. Metcalf,[5] F. A. Chudnovsky,[6] and E. A. Stern[7]

[1]*Department of Physics, University of Connecticut, Storrs, Connecticut 06269, USA*
[2]*Department of Physics, Yeshiva University, New York, New York 10016, USA*
[3]*Ceramics Division, National Institute of Standards and Technology, Gaithersburg, Maryland 20899, USA*
[4]*Department of Materials Science and Engineering, University of Maryland, College Park, Maryland 20742, USA*
[5]*Department of Materials Engineering, Purdue University, West Lafayette, Indiana 47907, USA*
[6]*Ioffe Physico-Technical Institute, St. Petersburg, Russia*
[7]*Department of Physics, Box 351560, University of Washington, Seattle, Washington 98195, USA*

(Received 4 October 2010; revised manuscript received 26 December 2010; published 18 February 2011)

X-ray diffraction and vanadium x-ray absorption near-edge structure (XANES) data have been obtained for $(V_{1-x}Cr_x)_2O_3$ samples containing several concentrations of Cr, crossing the metal-insulator transition boundary. For single-phase single-crystal samples our theoretical results are generally in good qualitative agreement with our experimental single-crystal XANES, for both crystal orientations relative to the incident-beam electric vector. However, an anomalous peak occurs for both orientations in the *K* pre-edge of the single-crystal sample containing 1.2% Cr, a paramagnetic insulator sample that is in the concentration regime corresponding to the room-temperature two-phase (coexistence) region of the phase diagram. Upon increasing the temperature of the 0.4% Cr powdered material to 400 K so that one enters the two-phase region of the phase diagram, a similar peak appears and then diminishes at 600 K. These results, as well as experiments done by others involving room-temperature and low-temperature XANES of a 1.1% Cr sample, suggest that this feature in the V pre-edge structure is associated with the appearance under some circumstances of a small amount of highly distorted VO_6 octahedra in the interface region between coexisting metal and insulating phases. Finally, we find that, for the two-phase regime, the concentration ratio of the metal-to-insulating phase varies between different regions from a sample batch of uniform composition made by the skull melting method.

DOI: 10.1103/PhysRevB.83.085105 PACS number(s): 71.30.+h, 61.05.cj, 61.05.cp, 78.70.Dm

I. INTRODUCTION

The metal-insulator transition (MIT) in Cr-doped V_2O_3, from a paramagnetic metal (PM) to a paramagnetic insulator (PI) at room temperature, has attracted much attention since it was discovered.[1] This interest is partly because both PM and PI phases were predicted to be metallic by band-structure calculations.[2,3] V_2O_3 is a corundum structure PM at room temperature and converts to a monoclinic antiferromagnetic insulator (AFI) when cooled to 155 K. On the other hand, the system $(Cr_xV_{1-x})_2O_3$, which converts from the PM state to the PI state at $x \approx 0.01$, maintains a corundum structure through the MIT.[1] In recent years, there have been significant theoretical and experimental advances in our understanding of this system. Held *et al.*[3] applied the local-density approximation–dynamical mean-field theory (LDA + DMFT) approach to the $(Cr_xV_{1-x})_2O_3$ system. These authors first applied the LDA to both pure V_2O_3 and $(Cr_xV_{1-x})_2O_3$ with $x = 0.038$. Using the LDA alone, both compositions were calculated to be metallic, a result that disagrees with experiment and is consistent with earlier calculations of Mattheiss.[2] In order to apply the full LDA + DMFT, Held *et al.*[3] then adjusted *U*, the Mott-Hubbard Coulomb interaction parameter, to obtain a reasonable splitting within the t_{2g} bands. The critical value for splitting of these levels comes out to be ∼5 eV. For *U* values of 4.5 eV, corresponding to a system in the PM phase on the threshold of transforming to the PI phase, the system is metallic. Furthermore, in the occupied states near the Fermi level this system is predicted to show a pronounced peak in the quasiparticle spectrum. Mo *et al.*,[4] using bulk-sensitive, high-energy photoemission as a probe, subsequently observed such a peak in the occupied density of states in metallic V_2O_3. This peak was observed somewhat above the transition temperature for transformation to the AFI state.[4] Similar high-energy photoemission experiments were then carried out for $(Cr_xV_{1-x})_2O_3$.[5] In agreement with theory, the quasiparticle peak detected for metallic V_2O_3 disappears for the PI phase material. However, for both the PI and AFI phases, the vanadium 3*d* parts of the photoemission spectra are not simple one-peak structures, and there is not a good theoretical understanding of these features.[5] In a recent investigation, Rodolakis *et al.*[6] have measured powder V *K*-edge x-ray absorption near-edge spectra (XANES) on $(Cr_xV_{1-x})_2O_3$ for *x* corresponding to 1.1% and 2.8% Cr concentrations. These experiments were conducted as a function of temperature and pressure and compare well to their theoretical calculations for the first and second pre-edge peaks. The authors also find that at an edge energy of ∼5472 eV, there is an enhanced intensity region for the sample with Cr composition 1.1% in the PI regime of the phase diagram, but not in the lower-temperature PM regime. For an interpretation of this effect, the authors refer to Gougassis *et al.*,[7] who discuss the *K*-edge XANES of NiO in terms of a theory involving nonlocal excitations. Rodolakis *et al.*[6] go on to demonstrate that the electronic properties of $(Cr_xV_{1-x})_2O_3$ can vary depending on the (pressure, concentration, temperature) route across the MIT boundary, and that the metallic phase reached by increasing pressure is different than a metallic phase obtained by changing doping or temperature.

The two-phase (coexistence) regime of the $(Cr_xV_{1-x})_2O_3$ system is of current interest. The existence of a two-phase region, containing both insulating and conducting phases, was reported by McWhan and Remeika in 1970,[1] based on powder x-ray diffraction (XRD) obtained at room temperature. By measuring relative peak intensities, McWhan and Remeika[1] obtained a dependence of the ratio of insulating (I) to conducting (M) phase on the concentration of Cr within the coexistence region at room temperature. For their conditions of sample preparation and thermal history, McWhan and Remeika[1] found that at room temperature a sample containing ~1% Cr would be PI, but would also contain mixed M and I phases. Based on these early results and interpretation, one infers that the PI nature of such a sample may be owing to the fact that the majority I phase prevents the minority M phase from spanning the sample so that a percolating metallic state cannot form. McWhan and Remeika[1] also found in a separate experiment that the room-temperature ratio of I to M phases within the coexistence concentration range can depend quite sensitively on the details of thermal history.

Subsequent to the earlier studies by McWhan and Remeika,[1] Jayaraman *et al.*[8] performed temperature-dependent powder XRD of $(Cr_xV_{1-x})_2O_3$ with $x = 0.006$, monitoring the (300) peak of the corundum structure. Only the M phase (300) peak was observed at room temperature, and only the I phase peak was observed at 503 K.[8] However, as the temperature was increased through the intermediate temperature coexistence regime, it was observed that the M peak systematically shifted toward the lower angle position of the (300) I peak so that at 473 K the M peak became a shoulder on the I phase peak. These authors attributed this effect to different thermal expansion coefficients between the conducting and insulating phases. To our knowledge, this explanation of the peak shift of the M peak toward the I phase peak as the concentration of the M phase decreases has not been tested experimentally.

In a recent theoretical study, Park *et al.*[9] applied cluster dynamical mean-field theory to the Mott transition. For their single-site calculation they derive a phase diagram that they remark "strongly resembles the phase diagram of Cr-doped V_2O_3." This phase diagram is divided up into five regions: bad metal, bad insulator, Fermi liquid, PI, and the coexistence (two-phase) region. For their plaquette calculation, the metallic state in the coexistence region differs from that in the pure Fermi-liquid region in featuring a quasiparticle peak that is broadened because of incoherence. The insulating state in the coexistence region has a smaller gap and differences in spectral characteristics relative to the case of a fully developed Mott insulator. For our purposes, the message of this recent calculation is that the electronic structure of $(Cr_xV_{1-x})_2O_3$ in the coexistence regime may be quite different than for the single-phase region. Hereafter we will refer to the phase diagram developed by Kuwamoto *et al.*,[10] which takes the hysteresis of this system, upon heating and cooling, into account, and includes the two-phase regime.

Previous calculations involving V K-edge XANES in systems related to $(Cr_xV_{1-x})_2O_3$ have been carried out by Meneghini *et al.*,[11] Joly *et al.*,[12] Cuozzo *et al.*,[13] and Rodolakis *et al.*[6] The calculations of Meneghini *et al.*[11] were devoted to *a-b* plane dichroism in the AFI phase. The calculations of Joly *et al.*[12] pertained to resonant x-ray scattering experiments in AFI V_2O_3. Cuozzo *et al.*[13] calculated the V K-edge absorption spectra of V_2O_3 using an 11-atom cluster. This last calculation does not distinguish between polarization directions in a single-crystal XANES experiment. The calculation by Rodolakis *et al.*[6] also concentrates on random powders and, for that reason, it does not offer results that differentiate between single-crystal orientations relative to the incident-beam electric vector.

In the present study, we performed powder XRD studies on $(Cr_xV_{1-x})_2O_3$, made by skull melting,[14] and have found that for samples in the two-phase concentration regime, the ratio of M to I phase varies between different crystal samples of the same composition. We have also investigated the V K-edge XANES for single-crystal and powder samples as a function of concentration x at room temperature as well as for specific concentrations of powder samples as a function of temperature. We have found that there is a pronounced peak C in the V K-edge single-crystal XANES of the material with $x = 0.012$, a composition that at room temperature is two phase. Our theoretical results are in reasonable agreement with our experiments for both crystal orientations for the single-phase materials, but not for peak C in the two-phase sample. This situation is similar to that reported by Rodolakis *et al.*[6] We have measured the region of peak C for concentrations other than those investigated in Ref. 6, and have found that peak C is absent both for pure single-phase metallic and single-phase insulator material, implying peak C has to do with the coexistence of two phases.[1]

The paper is organized as follows. Sec. II describes details about the preparation and characterization of the samples, and a brief description of the computational methods used. Results are presented in Sec. III. A discussion is given in Sec. IV. A summary and conclusions are presented in Sec. V.

II. EXPERIMENTAL AND COMPUTATIONAL METHODS

Single crystals of $(Cr_xV_{1-x})_2O_3$ with $x = 0$, 0.004, 0.012, 0.029, and 0.052 were prepared by the skull melting technique at Purdue University.[14] In addition, a single-crystal sample of pure V_2O_3, thin enough (15 μm) for transmission XANES, was manufactured and used for our pure V_2O_3 results.[15] The samples containing Cr were stoichiometric single crystals of high quality, which was confirmed by resistivity measurements, scanning electron microscopy, and XRD. In the pure V_2O_3, this was evident by resistivity measurements: (1) The resistivity dropped by seven orders of magnitude above T_c with a jump width of less than 0.2 K and a hysteresis loop width of 10 K, and (2) resistivity increased linearly with temperature in the metallic phase.[15]

For XRD studies, we used a Bruker diffractometer[16] operated in the "scissors mode," in which the powder sample remains fixed and both the x-ray source and detector move symmetrically to vary the Bragg angle. Under such conditions the powder in a specimen cannot move during a scan. A graphite monochromator was used to remove the copper $K\beta$ line from the XRD, but the copper $K\alpha_{1,2}$ doublet is unresolved. Single-crystal alignment and characterization was carried out with the aid of a gas area detector diffractometer (GADD).

V *K*-edge XANES data were obtained at the X-11A beam line at the National Synchrotron Light Source (NSLS). The beam line uses a double-crystal Si (111) monochromator, providing an energy resolution of $\Delta E/E = 10^{-4}$. The monochromator crystals were detuned 40% to reduce harmonics. For the single-crystal XANES on pure V_2O_3, thin (15-μm) crystals had the hexagonal *a*-*c* plane parallel to the sample surface and were measured in transmission mode at room temperature (PM) and 60 K (AFI). For single-crystal samples containing Cr, XANES data were obtained by using the glancing emergent angle (GEA) method, reported independently by Pease *et al.*[17] and by Suzuki,[18] to minimize the fluorescence distortion effect. Samples were aligned to have a flat (110) surface using GADD in order to obtain XANES for parallel and perpendicular orientations of an x-ray polarization vector relative to the crystal *c* axis. For the single-crystal sample with $x = 0.004$, however, the main edge V *K*-edge XANES was anomalously broadened in a manner that suggests the possibility of more than one *c*-axis direction. Here we do not publish or further analyze the single-crystal data from the $x = 0.004$ sample. Powder samples for transmission studies, measured at room temperature, were prepared by grinding and rubbing onto tapes by standard methods. For temperature-dependent measurements, powders were ground and mixed with a BN binder, then compressed into flat pellets. The samples were then heated in a furnace having a Kapton window, under flowing nitrogen.

The GEA method is used to reduce the overabsorption effect that arises in XANES studies of concentrated bulk samples measured by the fluorescence method. Some details of the GEA method need to be briefly reviewed. In the GEA mode, we used normal incidence to the crystal flat and, by blocking the beam to the ion chamber, restricted the detected fluorescence to a small angle, which in our case was of the order 3°. Because only a small solid angle of radiation can be used in GEA, GEA data from single crystals have enhanced the noise-to-signal ratio, relative to transmission powder results. In principle, the GEA method can never completely remove the fluorescence distortion. This assertion is evident in Ref. 17, in which it was shown that no matter how small the GEA angle, the fluorescence observed XANES from bulk copper always has a small, residual distortion relative to that observed using a copper foil in transmission. Recently, Frenkel *et al.*[19] compared single-crystal XANES obtained from single crystals of 2.9% Cr doped $(Cr_xV_{1-x})_2O_3$ with transmission powder XANES from the same material. To make this comparison, a composite single-crystal spectrum of 2/3 of the *E* perpendicular to the *c*-axis spectrum with 1/3 of the *E* parallel to the *c*-axis spectrum was compared to the powder transmission x-ray-absorption fine structure (XAFS).[19] The agreement was excellent. However, an unexplained aspect of this experiment was that the fine structure peaks were somewhat better resolved and stronger in the GEA than for the powder transmission data. This observation is opposite what is expected and is opposite to that observed for copper metal in Ref. 16. This finding implies that for the $(Cr_xV_{1-x})_2O_3$ system, some small unexplained distortion of the XANES is taking place that is associated with the manufacture of the powder sample itself.

Our computations were performed by the full multiple-scattering method within the Green's function formalism by a spin-polarized version of the XKDQ code.[20] Both dipole and quadrupole parts of electron-photon interaction were taken into account. Spectra were calculated using 51-atom clusters, and it was checked that an increase of cluster size up to 137 atoms does not change any features of XANES and pre-edge structure. The electron configurations of the absorbing atoms ($1s^1 3d^{2.9}$) included the 1*s* hole and additional 0.9 electrons at the 3*d* level as a screening charge. The exchange correlation potential was taken in the $X\alpha$ approach. To simulate a finite lifetime of electron-core excitation and experimental resolution, calculations were performed at a complex energy. Because the length of the photoelectron mean free path is not known for the low-energy region, the broadening of the spectra was calculated by employing a semiempirical energy dependence of the width of the electron-hole excited state. The resultant spectra are the averages of two calculations with the spin of the photoelectron being parallel and antiparallel to the spin of the absorbing atom. Calculations were carried out for pure V_2O_3, both in the PM and AFI structures, for both $E \parallel c$ and $E \perp c$ orientations of the XANES.

III. RESULTS

A. X-ray diffraction

Two kinds of XRD powder-diffraction scans were obtained. We obtained full-range scans that covered many peaks. Within the scatter of the data these scans were in agreement with the standard V_2O_3 pattern for the corundum structure, except that for samples with mixed conducting and insulating phase, some peaks were split. We also obtained data with a short angular range but better counting statistics in the vicinity of the (110) reflection (hexagonal indexing). All XRD data were obtained at room temperature (Fig. 1). The XRD corresponding to Fig. 1 were obtained less than 1 week after grinding single crystals to a powder. The pure V_2O_3 powder data was obtained from freshly ground single crystals of pure V_2O_3 prepared

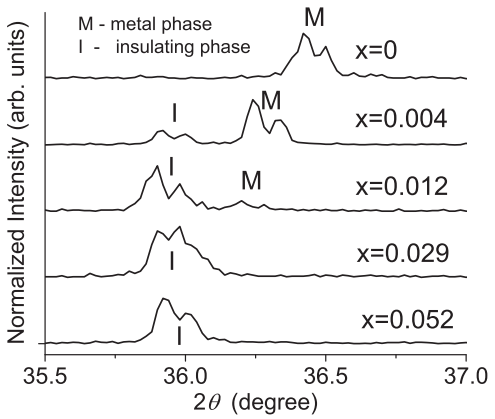

FIG. 1. XRD patterns of (110) reflection for powders ground from bulk crystals of $(Cr_xV_{1-x})_2O_3$ for various concentrations. All samples were measured within 1 week after grinding their respective single crystals. These XRD peaks all show the unresolved $K\alpha_{1,2}$ doublet, but the shape of the doublet is anomalous for the $x = 0.029$ sample. The curves are shifted vertically for clarity.

at Purdue University. All samples of this group correspond to either a single corundum phase $x = 0$ (PM), 0.029 (PI), and 0.052 (PI) or contain both metallic and insulating phases ($x = 0.004$, 0.012). We limit our discussion here to the scans in the vicinity of the strong (110) peak, obtained with better counting statistics. The (110) XRD of single-phase samples agree closely with results obtained by McWhan and Remeika.[1] As expected, we observe a shift in the a lattice parameter between the PM and PI phases. We obtain a value for the a parameter of 5.2% Cr in V_2O_3, which agrees within less than 0.01 Å of the McWhan-Remeika value of 5.00 Å. Our a value for pure V_2O_3 is ∼0.016 Å less than the McWhan-Remeika value of 4.95 Å. The powder camera values for the a parameter as obtained by McWhan and Remeika[1] are to be preferred to ours, and are obtained by a better technique for this particular purpose than use of our modern laboratory diffractometer.[21] In any case, these differences in the absolute value of the a parameter are not significant in the present context.

We noticed puzzling features in our XRD results for several compositions, as shown in Fig. 1:

(a) $x = 0.004$: In the phase diagram reported by Kuwamoto *et al.*,[10] a diagram that shows a region of thermal hysteresis between insulating and conducting phases, this composition is outside the two-phase region at room temperature. In our data a strong insulating phase $K\alpha_{1,2}$ doublet exists for the sample. From a measurement of the relative intensities between the M phase and the I phase peaks shown for this composition in Fig. 1, the concentration of the insulating phase in the sample is ∼26%. We speculate that the pronounced insulating phase fraction for a composition that is expected to be a pure conducting phase at room temperature may have to do with a rapid quench resulting from the skull melting procedure.

(b) $x = 0.012$: The concentration of PM in this sample appears to be ∼17%, which is significantly less than the value of 30% reported by McWhan and Remeika for this composition.[1] For the $x = 0.012$ concentration, the metallic phase peaks are significantly shifted to the lower-angle side relative to pure V_2O_3.

(c) $x = 0.029$: This sample has an anomalous shape of the XRD $K\alpha_{1,2}$ line. The composition should be a single-phase insulator according to the phase diagram.[10]

We obtained XRD from a second specimen with $x = 0.004$ to compare with the XRD of our first $x = 0.004$ specimen as shown in Fig. 1. Again, coexisting M and I phases were observed. However, the concentration ratio between the two phases was different between the $x = 0.004$ sample referred to in Fig. 1 and the second sample of the same $x = 0.004$ composition. We found variations in the ratio of the two phases between different samples of the $x = 0.012$ ingot as well. From the early results of McWhan and Remeika,[1] these results are not surprising. For samples with coexisting M and I phases, the ratio of I to M phase was found by McWhan and Remeika[1] to vary substantially with past thermal history, and it is quite conceivable that thermal history may vary from place to place within an ingot of these materials as made by skull melting.

Finally, we found that one sample of 1.2% Cr in V_2 O_3, when studied by a powder XRD experiment that commenced within a few minutes of grinding the crystal into a powder, changed its (110) XRD pattern slowly with time in an overnight scan. The intensity of the metallic phase $K\alpha_{1,2}$ doublet, relative to the insulating phase $K\alpha_{1,2}$ doublet, was initially large but decreased with time after grinding. An unexpected XRD feature observed only in the insulating phase $K\alpha_{1,2}$ doublet of this same powder sample also decreased with time after grinding. These were surprising observations, and although we have documented our results, we are not presently ready to present publishable data on the effect, because our overnight XRD spectrum on this sample comprises a time average of results. To study the effect rigorously, a synchrotron-based XRD experiment is required.

One conclusion we draw from these various XRD observations is that for samples in the coexistence (two-phase) concentration regime, the ratio of metallic to insulating phase can vary within a sample batch of uniform concentration of Cr, if the samples are made by skull melting.[14] As pointed out above, McWhan and Remeika[1] long ago found that the ratio of metallic to insulating phase for compositions within the two-phase region varies quite sensitively with the thermal history of the sample. Samples of similar two-phase compositions made by this same skull melting method have been used in many experiments by others, and thus our finding of a variation of the metallic-to-insulating phase ratio for two phase samples made by skull melting is therefore of interest in itself.

B. X-ray absorption near-edge structure

The energy scans of the absorption coefficients in the K-edge region for selected samples can be found in Ref. 19 and Fig. 6 below. Figures 2(a) and 2(b) focus on the V K pre-edge regions of the following single-crystal samples: AFI phase pure V_2O_3, PM phase pure V_2O_3, and PI phase $(V_{1-x}Cr_x)_2O_3$. For the PI phase samples we include room temperature data corresponding to $x = 0.012$, 0.029, and 0.052. Both polarization directions are included in the data. In agreement with Rodolakis *et al.*,[6] the pre-edge region features peaks A and B followed by structure C for the $x = 0.012$ sample. These details become more prominent after subtracting the base line.

All XANES figures below show absorption coefficient data normalized by the edge step. Peaks A and B vary more or less systematically with Cr concentration. This is not the case for the C structure. This structure has a maximum intensity for $x = 0.012$ (indicated by arrows) and is also weakly observable at $x = 0.029$ in the $E \perp c$ orientation. It is quite evident that this feature in the spectrum for $x = 0.012$, which is a mixture of M and I phases, cannot be represented as a linear combination of pure PM and pure PI XANES.

We then compare the XANES of three single crystals obtained by the GEA method, with transmission XANES for powder samples of the same compositions at room temperature. In crystals with trigonal symmetry, such as the PM phase of V_2O_3, simulated powder data can be compared to the weighted average of spectra of the two perpendicular orientations of the c axis (relative to the E vector). The $(1/3\,[E \parallel c] + 2/3[E \perp c])$ spectra of single crystals and spectra of powder samples are superimposed in Fig. 3. This method is only an approximation, even for the perfect crystals, because it assumes that x-ray absorption

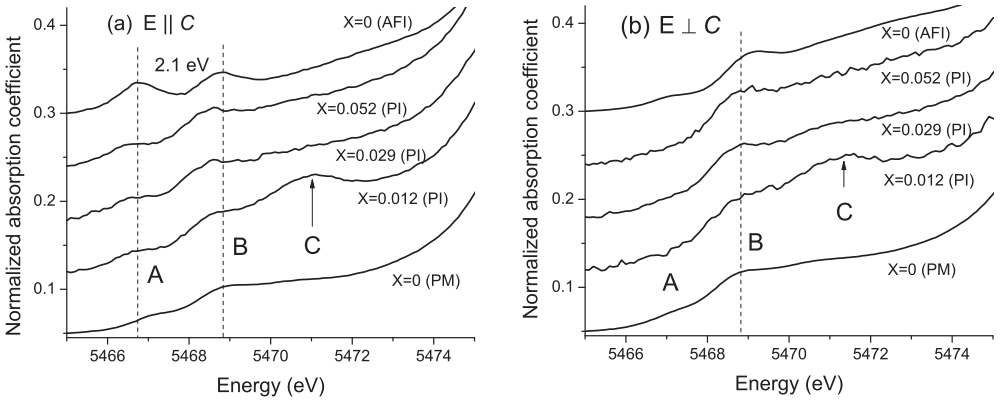

FIG. 2. Polarization-dependent V *K*-edge XANES obtained for single crystals of $(Cr_xV_{1-x})_2O_3$. The polarization vector is (a) parallel and (b) perpendicular to the hexagonal *c* axis. The curves are shifted vertically for clarity.

cross-section is dominated by dipole contribution only. We note, however, that the pre-edge features are caused also by quadrupole contributions, and their angular dependence should be different from the one dictated by the dipole contribution only. This complication may contribute to slight discrepancies between single-crystal and powder data for peaks *A* and *B* region in Fig. 3. These discrepancies are much smaller than the pronounced enhancement of peak *C* for the two-phase samples, which are the subject of this study. This issue is discussed further in Sec. IV.

It may be seen that pre-edge structure features are nearly consistent between single-crystal and powder data, except for the region of peak *C* for the two-phase sample $x = 0.012$ and the region of peak *C* for the sample with $x = 0.029$. The data are also completely consistent in the region of the main edge. We note that in the powder data of Rodolakis *et al.*,[6] for their $x = 0.011$ sample, the *C* region is different than the one we observe for our $x = 0.012$ powder data. In the former work done with the $x = 0.011$ powder sample, peak *C* is somewhat enhanced relative to the one we observe for our $x = 0.012$ sample. This enhancement might be caused by a different thermal history during skull melting of our sample relative to that of the sample of Rodolakis *et al.*[6]

Finally, we studied the temperature-dependent XANES of the $x = 0$, 0.004, and 0.052 powder samples (Fig. 4 below). For all temperatures studied, a pure V_2O_3 sample remains in the PM phase whereas the $x = 0.052$ sample remains in the PI phase. For both these single-phase samples, the amplitudes of peaks *B* and *C* monotonically increase with temperature. For $x = 0.004$, the phase diagram of Kuwamoto *et al.*[10] indicates that the composition is just at the border of a two-phase region of the phase diagram, which exists between $T \sim 350$ and 450 K.

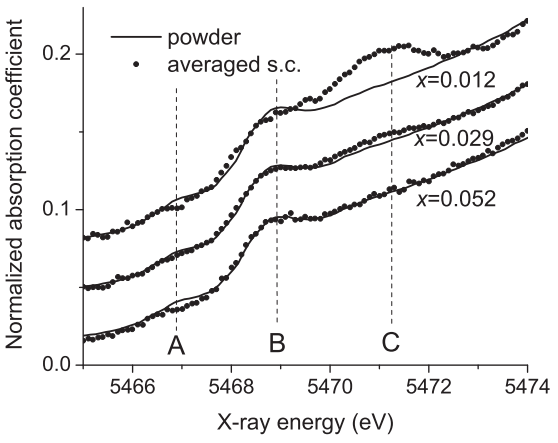

FIG. 3. Comparison of the orientationally averaged V *K* pre-edge data obtained for $(Cr_xV_{1-x})_2O_3$ single crystals and powder samples obtained by grinding single crystals of the same composition. Note the dramatic enhancement of feature *C* in the single crystal relative to the powder for the composition corresponding to the mixed phase ($x = 0.012$). A much smaller enhancement is also noticeable for the $x = 0.029$ sample. The curves are shifted vertically for clarity.

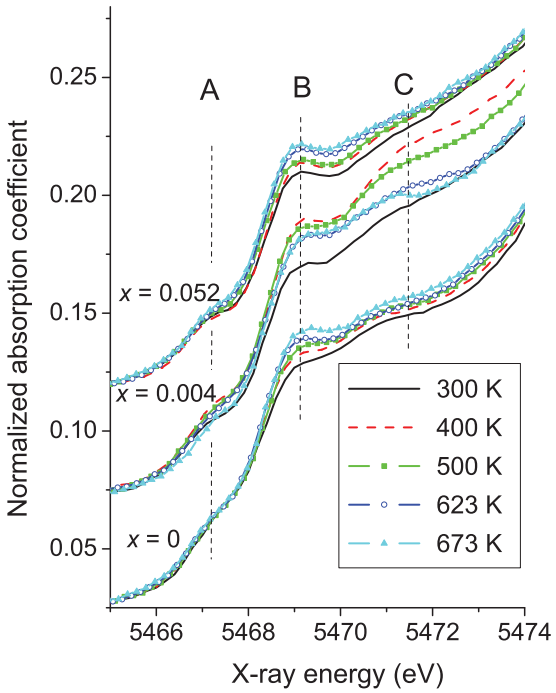

FIG. 4. (Color online) Temperature dependence of the V *K*-edge XANES data obtained for $(Cr_xV_{1-x})_2O_3$ powders. Features *A*, *B*, and *C* change monotonically with temperature for single-phase ($x = 0$ and $x = 0.052$) concentrations. Note the nonmonotonic behavior of peak *C* for the mixed-phase region in the $x = 0.004$ sample. The curves are shifted vertically for clarity.

Such a high-temperature two-phase region was experimentally observed by Jayaraman *et al.*[8] for a sample with $x = 0.006$. The most prominent feature of the temperature dependence of this spectrum is that the intensity of the structure *C* abruptly increases when the temperature changes from ambient to 400 K. The 400 K temperature is the only temperature investigated in this study that belongs to the two-phase region of the diagram. When the temperature increases from 400 to 500 K the intensity of the structure *C* slightly decreases but still is considerably greater than for the other three temperatures. After an increase of the temperature up to 623 K, structure *C* returns to a magnitude that is typical for a one-phase sample. These results are shown in Fig. 4.

C. Photoemission

Our investigation into the XRD of different sections of single crystals of the same composition, in the coexistence regime, was motivated by an interesting situation that has arisen with regard to recent photoemission studies carried out by others.[5] These studies are now briefly discussed. We noticed that one of the samples investigated by Mo *et al.*[5] was 1.2% Cr-doped V_2O_3 at room temperature. For this composition, using their sample synthesis methods, McWhan and Remeika[1] report a fully 30% conducting phase in a predominantly insulating matrix. Because recent studies show that metallic phases in the Cr-doped V_2O_3 system show a quasiparticle peak spectral shape in photoemission, and insulating phases do not, then in one simple interpretation of previous evidence, there could be a mixture of a 30% quasiparticle peak spectrum and a 70% insulator spectrum in the photoemission of material with 1.2% Cr at room temperature. We simulated such a spectrum assuming a 20% metallic and a 80% insulating phase, as shown in Fig. 5 (narrow line). No such experimental spectrum has been observed. This finding leads us to explore how much variation there might actually be between the conducting and insulating phase ratios within a sample batch of uniform Cr concentration. We found that for samples of the same composition of $x = 0.012$, there can be markedly differing ratios of *M* to *I* phases within different regions of the same ingot as made by skull melting. It would be of interest to investigate such a photoemission spectrum on a single-crystal specimen that is known to have a substantial fraction of metallic phase mixed into the predominantly insulating phase.

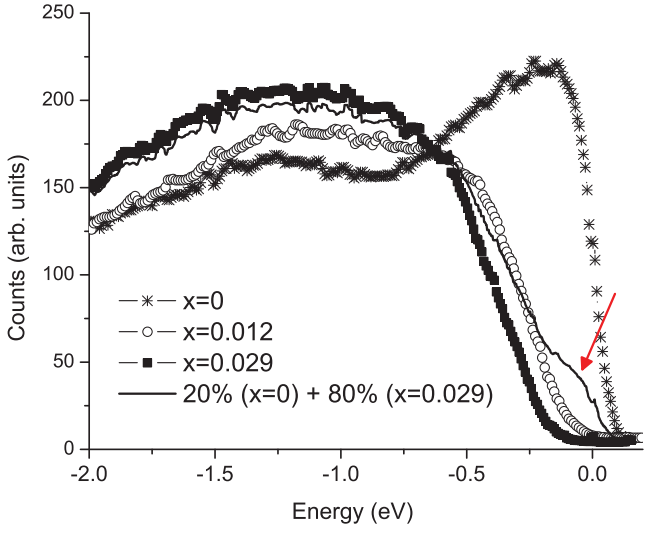

FIG. 5. (Color online) Simulated spectrum from photoemission (Ref. 5) for an 80% fully *I* phase (2.9% Cr), and a 20% fully *M* phase (pure PM phase V_2O_3). The simulated spectrum (solid line) shows a strong high-energy feature (arrow), not seen in the experimental curve for a two-phase room-temperature material with $x = 0.012$.

IV. DISCUSSION

An interesting interpretation of the pre-edge structure in V *K* XANES was given by Rodolakis *et al.*[6] by studying powdered samples. In the present paper, we report on the comparison of the single-crystal and powder measurements that allowed us to take another look at the origin of the pre-edge structure by contrasting these two types of samples.

First, let us describe the lowest vacant electronic states of the V_2O_3 corundum crystal, which determine the structure of the pre-edge region, within a simple one-electron approach, neglecting electron correlation. Antibonding hybridized V 3*d*-O 2*p* orbitals in an ideal [VO_6] octahedron split into lower t_{2g} orbitals and upper e_g. A trigonal "umbrella" distortion of those octahedra in the V_2O_3 corundum lattice breaks the inversion symmetry, transforming the e_g representation to e^σ, and further splits the t_{2g} representation into a and e^π. The superscripts σ and π on e denote the type of hybridization of the corresponding atomic orbitals. It is worth noting that the hybridization of V 3*d* with O 2*p* orbitals for e^σ representation is more intensive than for the e^π case.

Information from the literature regarding the values of the t_{2g}-e_g and the following $a - e^\pi$ splittings seems somewhat controversial. In the framework of a semiempirical crystal-field split approach, Rodolakis *et al.*[6] used 2 and 0.3 eV, whereas Park *et al.*[22] used 1 and 0.05 eV, respectively. Our FMS calculations result in 1.8 and 0.01 eV. Despite these discrepancies, one can state that the trigonal splitting of the t_{2g} states is negligible in comparison with the width of even the lowest-energy pre-edge peak *A*.

According to the final-state rule,[23] the Hamiltonian employed for the calculations of the XANES includes the potential of the properly screened core hole. This attractive potential shifts localized V 3*d* states down by ~2 eV. As a result, in the PM insulators, antibonding t_{2g} and sometimes e_g states of an absorbing TM atom appear to be well below the bottom of the conduction band. That is why the pre-edge peaks corresponding to the excitation of the core electron to these states are often called x-ray excitons.

There is a consensus now that the electron configuration of the ground state of the vanadium ion in V_2O_3 is a triplet formed by the superposition of the $(e^\pi\uparrow, e^\pi\uparrow)$ and $(a\uparrow, e^\pi\uparrow)$ two-electron states.[6,22] Therefore, as it was pointed out by Rodolakis *et al.*,[6] the lowest-energy pre-edge peak *A* corresponds to an x-ray exciton with three t_{2g} electrons in high-spin configurations, $(a\uparrow, e^\pi\uparrow, e^\pi\uparrow)$ or $(e^\pi\uparrow, e^\pi\uparrow, e^\pi\uparrow)$.

The value of the t_{2g}-e_g crystal-field splitting corresponds to the energy separation between peaks *A* and *B*. Therefore, excitation of the 1*s* electron to $e^\sigma\uparrow$ contributes to peak *B*. The magnitude of the exchange interaction for V^{+3} is also ~2 eV. Hence the transitions to $t_{2g}\downarrow$ are the second part of the

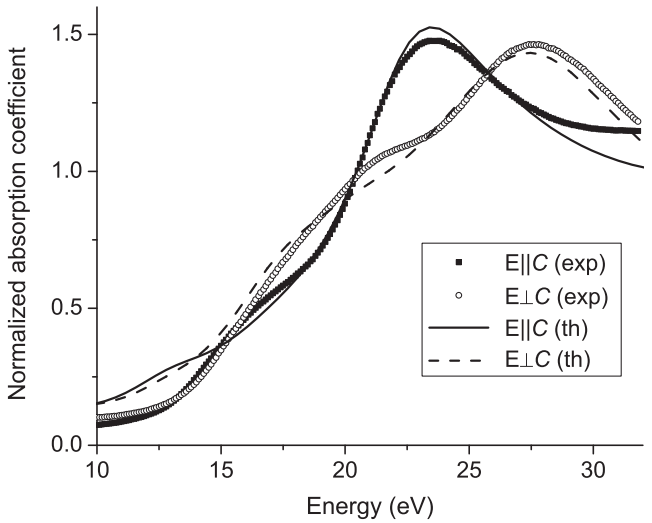

FIG. 6. Comparison of experimental and calculated spectra for the main edge region in V_2O_3 single crystals for two different orientations of the x-ray polarization vector. The data were taken in fluorescence at room temperature.

contribution to peak *B* whereas transitions to $e^{\sigma}\downarrow$ contribute to a broad structure *C*. At first glance it is strange that the structure *C* is so weak at room temperature for most samples. In many octahedrally coordinated TM oxides with metal ions in both $3d^0$ and PM states, there are peaks in the pre-edge structure caused by excitation of photoelectrons to the 3*d* states of neighboring metal atoms. There could be two reasons that suppress displaying these transitions as a pronounced peak: (1) There are too many different final states that make this structure quite broad. (2) The low-energy photoelectron free path is too short in V_2O_3, which also smears the structure. (The origin of the *C* structure in the spectra of the $x = 0.012$ single-crystal sample and the $x = 0.004$ powder sample at 400 K will be discussed separately.)

The interpretation of the pre-edge structure given above is confirmed by calculations presented in Figs. 6 and 7. The energy scale, unique for all calculated spectra, was aligned with that for experimental data to achieve the best agreement in the range of the main edges. The agreement between calculated and experimental spectra in the main edge region (Fig. 6) is excellent for both polarization directions. Calculations of the pre-edge yield quite reasonable energies and amplitudes for peaks *A* and *B* (Fig. 7). One can see that peak *A* in some calculated spectra is more intense than in the experimental ones. We point out two further issues that affect comparison between theory and experiment.

First, the quadrupole contributions to pre-edge peaks can cause the intensities of these features to be dependent on the direction of the x-ray *k* vector for single-crystal XANES. The theoretical calculation of this angular dependence requires experimental input not available to us. Brouder has shown[24] that accurately angular-resolved data must be obtained for several different *k*-vector directions in order to analyze the quadrupole contribution. Our experimental studies were carried out for the purpose of obtaining not only XANES but also extended XAFS (EXAFS) so that the great majority of data collection was by necessity on regions of the x-ray absorption spectra that are described accurately by the dipole approximation alone. We have, however, calculated the maximum angular variation owing to the quadrupole contribution, and found that these variations are considerably less intense that the pronounced *C* structure enhancement observed in the two-phase state, which is the main topic of this study.

Second, the one-electron multiple-scattering approach calculates the transition rate on both vacant and occupied electron states; hence our calculations correspond to transitions to completely empty t_{2g} states, whereas two of these states are occupied.

In principle, the angular dependence of the pre-edge peak *A* gives an opportunity to determine experimentally the electron configuration of the ground state. The ground-state configuration determines the weights with which 1*s* electron excitations to *a* and e^{π} final states contribute to peak *A* intensity. Because the probabilities of the $1s \rightarrow a$ and $1s \rightarrow e^{\pi}$ transitions are different and can be calculated theoretically for a given atomic configuration for every polarization and wave-vector direction, the measured angular dependence enables one to determine the weights. As was mentioned earlier, both dipole and quadrupole parts of the electron-photon interaction contribute to peak *A* intensity. In slightly distorted $[TMO_6]$ octahedral, the quadrupole part practically does not depend on the octahedron distortion. In contrast, the dipole contributions caused by

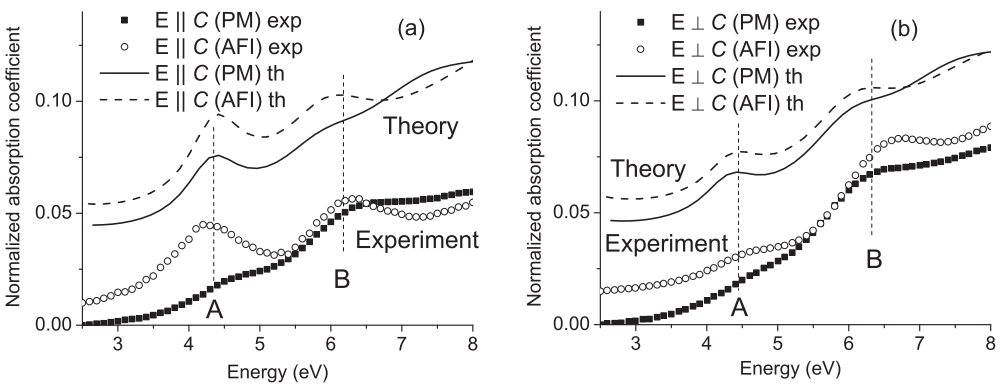

FIG. 7. Pre-edge regions in the polarization-dependent V *K* edge in V_2O_3. Shown are the data (symbols) and theory (lines) for the AFI and PM phases. The curves are shifted vertically for clarity.

the *p-d* mixture owing to breaking the central symmetry strongly depend on the instantaneous local atomic structure. The determination of the ground state is beyond the scope of the present article.

Another confirmation of our interpretation of the pre-edge peaks is given by the temperature dependence of pre-edges for pure V_2O_3 and $x = 0.052$ powder samples as shown in Fig. 4. Both samples exhibit a monotonic increase of *B* and *C* intensities with a temperature increase and do not change outside these regions. Because both samples remain in the single-phase states through the whole temperature interval studied, the only change of the atomic structure, except for a weak increase of the lattice constants, is the growth of the amplitude of temperature vibrations, which in turn results in an increase of the mean-squared displacement of the V atom from the instantaneous center of an oxygen octahedron. It was shown both experimentally and theoretically that such an increase results in an enhancement of the pre-edge peaks that are caused by photoelectron excitation of the e_g states. This effect has been observed previously in a number of crystals with octahedrally coordinated PM TM ions $EuTiO_3$ and $SrTiO_3$.[25,26] Because in V_2O_3, transitions to the e^σ states contribute to both *B* and *C* peaks, both of them enhance with an increase in temperature. We illustrate our conclusion by a simple simulation of the effects of thermal vibration. We calculated the V pre-edge in the same 51-atom cluster but with absorbing V ions being displaced, in turn, toward each of the neighboring O atoms by 0.06 Å. The average of these calculations is shown in Fig. 8.

In conclusion, we will offer a speculative model for the appearance of peak *C* in the spectra of an $x = 0.012$ single crystal and the "anomalous" temperature dependence of the same region for an $x = 0.004$ single crystal. First, note that, according to Kuwamoto *et al.*,[10] $x = 0.012$ is the only two-phase sample at room temperature among those studied, whereas the $x = 0.004$ powder sample crosses the two-phase region during heating. Second, the vanadium *K* pre-edge structure in V_2O_5 crystal, $VOPO_4$ xerogel, and other

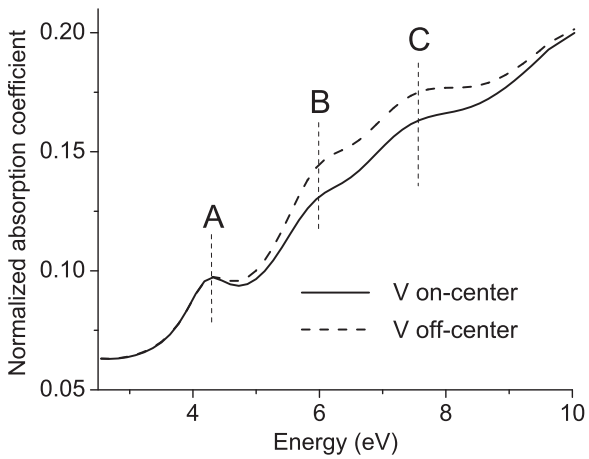

FIG. 8. Theoretical calculations of angular-averaged, pre-edge features carried for undistorted (solid lines) and distorted (dashed lines) configurations of the local V environment in V_2O_3. Distortions were introduced by displacing V atoms in the simulated cluster toward the nearest O atoms.

compounds with vanadium ions in highly distorted oxygen octahedral environments, contain an intense peak with a magnitude close to the main edge step.[27–30] The energy of this peak coincides with that of the *C* peak in the $x = 0.012$ sample spectrum, but the area under the peak in V_2O_5 exceeds that in the $x = 0.012$ sample by ~100 times. A possible explanation of the peak C origin in the $x = 0.012$ single crystal is that, after two-phase crystal quenching, ~1% of V atoms placed on the phase boundaries appear in distorted environments, owing to the different structures of the coexisting PI and PM regions, and produce corresponding contributions to the *C* peak. This distorted part of the crystal structure creates strain that releases when the crystal is ground during powder sample preparation; regular oxygen octahedra restore, and therefore the *C* peak may diminish in an $x = 0.012$ powder sample spectrum relative to the single crystal. We point out that Rodolakis *et al.*[6] observe an enhanced intensity of the peak *C* region for a powder sample with $x = 0.012$, but this peak *C* disappears when the sample is lowered in temperature so that it is single phase. However, the intensity of peak *C* in the room-temperature powder sample with $x = 0.012$ observed by Rodolakis *et al.*[6] is much less than what we observe for our single-crystal sample of the same composition. Furthermore, when our $x = 0.004$ powder sample is heated and crosses the two-phase region, a small fraction of V ions also appears in a highly distorted environment that, again, results in a distortion of the *C* structure in the pre-edge. When the temperature exceeds 600 K and the sample again falls into the one-phase region, the usual pre-edge structure restores, but with enhanced magnitudes of the *B* and *C* peaks, as in the cases of the $x = 0$ and 0.052 powder samples.

Our analysis, cumulatively, indicates the existence of distorted structures in a mixed-phase single crystal. We also found that, in one case, when the XRD was observed within minutes of grinding the single crystal to a powder, the XRD pattern changed with time overnight. A possible explanation is that there can be metastable phases related to the coexistence of two types of environments, and the grinding relieves internal stresses. Furthermore, if there is a mixture of *M* and *I* phases, because the pure *M* and pure *I* phases have quite different c/a ratios, then the interfacial region between the two different crystal structures would be expected to be disordered, and it is possible that distorted VO_6 octahedra could result along the interfacial surfaces. Wong *et al.*[30] carried out a careful study of the XANES for several oxides of V, but their graphical data is not published on a large enough scale to view the pre-edge structures well. On the other hand, Vining *et al.*[31] have made a direct comparison of the XANES of V_2O_5 and PM V_2O_3. From this comparison it may be seen that peak *C* observed both by us and Rodolakis *et al.*,[6] in a composition with $x = 0.011$ or $x = 0.012$ (present study), is located rather close in energy to the position of the major XANES peak observed by Vining *et al.*[31] for V_2O_5. The V_2O_5 structure contains a markedly distorted VO_6 octahedron that results in a pronounced XANES peak that is just at the energy of our large peak in single crystal, 1.2% Cr-doped V_2O_3, supporting our suggestion that it is such distorted octahedra at the interface between two different crystal structures in the two-phase samples that give rise to the enhanced peak *C*. It is also interesting to note that, experimentally, as one decreases the Cr composition from the pure *I* regime at room temperature toward the mixed *I* and *M*

phase regime ($x = 0.029$), a precursor of peak *C* is observed, but only for the electric vector perpendicular to the *c*-axis orientation.

V. SUMMARY AND CONCLUSIONS

We have obtained V *K*-edge XANES for a series of single-crystal specimens of $(Cr_xV_{1-x})_2O_3$, for various Cr concentrations. For Cr concentrations corresponding to single-phase material according to the phase diagram of Kuwamoto *et al.*,[10] two pre-edge features we call peaks *A* and *B* vary systematically with concentration, and show a dependence on the orientation of the photon electric vector direction that agrees approximately with theory. On the other hand, there is a pronounced peak *C* for both polarization directions in the XANES of a sample with $x = 0.012$, which is expected to be in the two-phase "coexistence" regime at room temperature. This peak occurs at ~5471 eV. We observe a much weaker enhancement of the XANES in this energy region for a sample with $x = 0.029$, for one orientation only of the electric vector. We point out that peak *C* is associated with the two-phase, or coexistence, regime of the $(Cr_xV_{1-x})_2O_3$ system, which is characterized by coexisting metal and insulating phases with different crystal structures. Thus, the feature diminishes or disappears for Cr concentrations corresponding to the single-phase regions of the phase diagram. We find that if we increase systematically the temperature of a powder specimen of $x = 0.004$ material from room temperature to 630 K, for intermediary temperatures near the two-phase region of the phase diagram, a peak near 5471 eV develops, and then the peak diminishes when the temperature is again in a single-phase region.

We propose a model for peak *C*. We point out that the energy position of this feature is close to that expected for the V *K*-edge XANES of V atoms in strongly distorted VO_6 polyhedra, such as are found in V_2O_5 or xerogel.[27,30] This feature is found to be so pronounced in these materials that only ~1% of V atoms in such a polyhedral would markedly effect the V *K*-edge XANES. We suggest that in the coexistence regime, the interface between insulating and metallic phases will be markedly strained, and that this strain is associated with peak *C*.

As part of our sample characterization, we have also determined that for samples in the two-phase, or coexistence, concentration region as made by skull melting, the ratio of metal-to-insulating phase concentration varies markedly from region to region for material with a uniform Cr concentration. This finding is completely to be expected based on old studies by McWhan and Remeika,[1] if indeed different portions of an ingot of $(Cr_xV_{1-x})_2O_3$ as made by skull melting cool down with different thermal histories. For one sample with $x = 0.012$, we observed that a powder specimen observed within a few minutes of grinding from a single crystal exhibited an XRD pattern that changed systematically overnight. Other investigators have used samples of nearly the same composition, made by the same skull melting method, and therefore, these complications of the XRD interpretation apply to other experiments besides those reported here. In particular, if a room-temperature PI sample with $x = 0.012$ were to have a 30% concentration of the metallic phase, as was reported for one of the specimens studied by McWhan and Remeika,[1] in a simple model one would expect a noticeable quasiparticle peak in photoemission, where we point out that, in fact, so far none is observed (Fig. 5).

Finally, we point out that the two-phase region of this system is not only of fundamental interest, as pointed out by the theory of Park *et al.*[9] The ratio between the metallic and insulating phases in the coexistence region can depend on thermal history, and we find evidence that interfacial strains between the coexisting phases in the coexistence region of the phase diagram can have pronounced effects. Because any device that uses the $(Cr_xV_{1-x})_2O_3$ system as a switch of some sort by changing between the PI and PM states would be influenced by changes in the ratio of phases and consequent changes in interfacial strains as one traverses the coexistence region, our findings may have device implications.

ACKNOWLEDGMENTS

The authors acknowledge support by the US Department of Energy Grant No. DE-FG05ER36184.The NSLS is supported by the Divisions of Materials and Chemical Sciences of Department of Energy. PNC/XOR is supported by the US Department of Energy, NSERC of Canada, University Washington, Simon Fraser University, Pacific Northwest National Laboratory, and the Advanced Photon Source is supported by the US Department of Energy under Contract No. W-31-109-Eng-38. We appreciate the support of the Institute of Materials Science (I.M.S.) of the University of Connecticut, and are grateful to J. Gromek of I.M.S. for his expert assistance with the laboratory x-ray equipment.

*pease@ims.uconn.edu
†anatoly.frenkel@yu.edu
‡victor.krayzman@nist.gov

[1] D. B. McWhan and J. B. Remeika, Phys. Rev. B **2**, 3734 (1970).
[2] L. F. Mattheiss, J. Phys. Condens. Matter **6**, 6477 (1970).
[3] K. Held, G. Keller, V. Eyert, D. Vollhart, and V. I. Anisimov, Phys. Rev. Lett. **86**, 5345 (2001).
[4] S. K. Mo, J. D. Denlinger, H. D. Kim, J. H. Park, J. W. Allen, A. Sekiyama, A. Yamasaki, K. Kadono, S. Suga, Y. Saitoh, T. Muro, P. Metcalf, G. Keller, K. Held, V. Eyert, V. I. Anisimov, and D. Vollhardt, Phys. Rev. Lett. **90**, 186403 (2003).
[5] S. K. Mo, H. D. Kim, D. D. Denlinger, J. W. Allen, J. H. Park, A. Sekiyama, A. Yamasaki, S. Suga, Y. Saitoh, T. Muro, and P. Metcalf, Phys. Rev. B **74**, 165101 (2006).
[6] F. Rodolakis, P. Hansmann, J. P. Rueff, A. Toschi, M.W. Haverkort, G. Sangiovanni, A. Tanaka, T. Saha-Dasgupta, O. K. Anderson, K. Held, M. Sikora, I. Alliot, J. P. Itie, F. Baudelet, P. Wzietek, P. Metcalf, and M. Marsi, Phys. Rev. Lett. **104**, 047401 (2010).
[7] C. Gougoussis, M. Calandra, A. Seitsonen, C. Brouder, A. Shukla, and F. Mauri, Phys. Rev. B **79**, 045118 (2009).

[8]A. Jayaraman, D. B. McWhan, J. P. Remeika, and P. D. Dernier, Phys. Rev. B **2**, 3751 (1970).
[9]H. Park, K. Haule, and G. Kotliar, Phys. Rev. Lett. **101**, 186403 (2008).
[10]H. Kuwamoto, J. M. Honig, and J. Appel, Phys. Rev. B **22**, 2626 (1980).
[11]C. Meneghini, S. D. Matteo, C. Monesi, T. Neisius, L. Paolasini, S. Mobilio, C. R. Natoli, P. A. Metcalf, and J. M. Honig, Phys. Rev. B **72**, 033111 (2006).
[12]Y. Joly, S. Di Matteo, and C. R. Natoli, Phys. Rev. B **69**, 224401 (2004).
[13]M. Cuozzo, Y. Joly, E. K. Hlil, and C. R. Natoli, in *Theory and Computation for Synchrotron Radiation Spectroscopy*, edited by M. Benfatto, C. R. Natoli, and E. Pace (AIP, Melville, NY, 2000), p. 45.
[14]P. Metcalf and J. Honig, Curr. Top. Cryst. Growth Res. **2**, 445 (1995).
[15]A. I. Frenkel, E. A. Stern, and F. A. Chudnovsky, Solid State Commun. **102**, 637 (1997).
[16]Certain commercial equipment or instruments are identified in this document. Such identification does not imply recommendation or endorsement by the National Institute of Standards and Technology, nor does it imply that the products identified are necessarily the best available for the purpose.
[17]D. M. Pease, D. L. Brewe, Z. Tan, and J. I. Budnick, Phys. Lett. A **138**, 230 (1989).
[18]Y. Suzuki, Phys. Rev. B **39**, 3393 (1989).
[19]A. I. Frenkel, D. M. Pease, J. I. Budnick, P. Shanthakumar, and T. Huang, J. Synchrotron Radiat. **14**, 272 (2007).
[20]R. V. Vedrinskii, V. L. Kraizman, A. A. Novakovich, P. V. Demekhin, and S. V. Urazhdin, J. Phys. Condens. Matter **10**, 9561 (1998).
[21]L. V. Azaroff, *Elements of X-Ray Crystallography* (McGraw-Hill, New York, 1968).
[22]J. H. Park, L. H. Tjeng, A. Tanaka, J. W. Allen, C. T. Chen, P. Metcalf, J. M. Honig, F. M. F. de Groot, and G. A. Sawatzky, Phys. Rev. B **61**, 11506 (2000).
[23]U. von Barth and G. Grossmann, Solid State Commun. **32**, 645 (1979).
[24]C. Brouder, J. Phys. Condens. Matter **2**, 701 (1990).
[25]B. Ravel, E. Stern, R. Vedrinskii, and V. Kraizman, Ferroelectrics **206**, 407 (1998).
[26]B. Ravel, Ph.D. dissertation, University of Washington, 1997.
[27]B. Poumellec, V. Kraizman, Y. Aifa, R. Cortès, A. Novakovich, and R. Vedrinskii, Phys. Rev. B **58**, 6133 (1998).
[28]S. Nozawa, T. Iwazumi, and H. Osawa, Phys. Rev. B **72**, 121101(R) (2005).
[29]B. Poumellec, V. Kraizman, Y. Aifa, and R. Cortez, Phys. Rev. B **58**, 6133 (1998).
[30]J. Wong, F. W. Lytle, R. P. Messmer, and H. W. Maylotte, Phys. Rev. B **30**, 5596 (1984).
[31]W. Vining, A. Goodrow, J. Strunk, and A. T. Bell, J. Catal. **270**, 163 (2010).